Modal analysis and suppression of the Fourier modal method instabilities in highly conductive gratings

Nikolay M. Lyndin,[1,*] Olivier Parriaux,[2] and Alexander V. Tishchenko[2]

[1]*Institute of General Physics, Vavilova Street 38, 119991 Moscow, Russia*
[2]*Laboratoire Hubert Curien UMR CNRS 5516 (formerly LTSI), Université Jean Monnet, 18 Rue Benoît Lauras, 42000 Saint-Etienne, France*
**Corresponding author: lyndin@ran.gpi.ru*

Received August 20, 2007; revised September 25, 2007; accepted September 27, 2007; posted October 19, 2007 (Doc. ID 86573); published November 21, 2007

The Fourier modal method (FMM), often also referred to as rigorous coupled-wave analysis (RCWA), is known to suffer from numerical instabilities when applied to low-loss metallic gratings under TM incidence. This problem has so far been attributed to the imperfect conditioning of the matrices to be diagonalized. The present analysis based on a modal vision reveals that the so-called instabilities are true features of the solution of the mathematical problem of a binary metal grating dealt with by truncated Fourier representation of Maxwell's equations. The extreme sensitivity of this solution to the optogeometrical parameters is the result of the excitation, propagation, coupling, interference, and resonance of a finite number of very slow propagating spurious modes. An astute management of these modes permits a complete and safe removal of the numerical instabilities at the price of an arbitrarily small and controllable reduction in accuracy as compared with the referenced true-mode method. © 2007 Optical Society of America

OCIS codes: 050.1950, 050.1960.

1. INTRODUCTION

The Fourier modal method (FMM) has been considered as a simple and efficient tool for one-dimensional (1D) gratings analysis since 1996 when the problem of TM incidence on gratings was given a sound solution [1–3]. Numerical studies have shown that the FMM can deal efficiently with low-loss metals in the visible wavelength range [4,5]. However, the method still faces difficulties when used in silver, gold, or copper gratings further in the infrared. Popov *et al.* [6] have shown in a case study that the numerical results given by the FMM exhibit strong and unpredictable instabilities. These were attributed to the imperfect conditioning of the matrices to be diagonalized. This statement was later questioned by Watanabe [7]. A heuristical solution was proposed to introduce artificial metal losses in order to damp the instabilities and/or to apply two-step truncation [6]. Such strategy amounts to treating a different although neighboring electromagnetic problem.

The present paper undertakes the analysis of the test structure considered in [6,7] from a modal standpoint. The source of instability will be identified as the excitation of high-order spurious modes generated by the truncation of the Fourier series representing the Maxwell equations. These modes will then be shown to possibly lead to high-contrast interferences of very high sensitivity on the optogeometrical parameters of the excited structure. Finally, an astute mode-filtering operation will make the transformation of the mathematically exact but numerically highly sensitive solution of the truncated Fourier representation of Maxwell's equations into a nearly exact and stable solution. This analysis will not be made from a mathematical standpoint. We will explore the very grating structure analyzed in [6,7] and bring as much as possible a qualitative physical insight to its numerical analysis. The FMM was implemented with its last known development into an existing set of grating modeling codes. As in [6], the method that is used as the reference is the true-mode method (TMM) [8,9] with its most recent developments [10]. This gives us confidence that the comparison is made in the best common-mode conditions.

2. FOURIER MODES

The binary grating is illuminated by a TM polarized plane wave (the H field is parallel to the grating grooves) under the incidence angle θ. Figure 1 reproduces the numerical results obtained in [7] for a highly conductive grating made of a lossless metal with $n_s=0+i10$. The minus-first-order diffraction efficiency is computed by the FMM as a function of the air gap between the metal walls of the grooves. The values of the parameters are the same as in [7]. The grating period Λ and depth are 500 nm, the wavelength λ is 632.8 nm, and the incidence angle θ is 30°. The curve of Fig. 1 is obtained with a number $N=31$ of diffraction orders (truncation number), which defines the $N \times N$ matrix to be diagonalized. The FMM mathematical treatment is made according to [2]. The efficiency is calculated for 1001 values of the groove width from 10 nm to 490 nm with constant interval. As already shown in [6], the FMM results appear as a noise on the

 © 2007 Optical Society of America

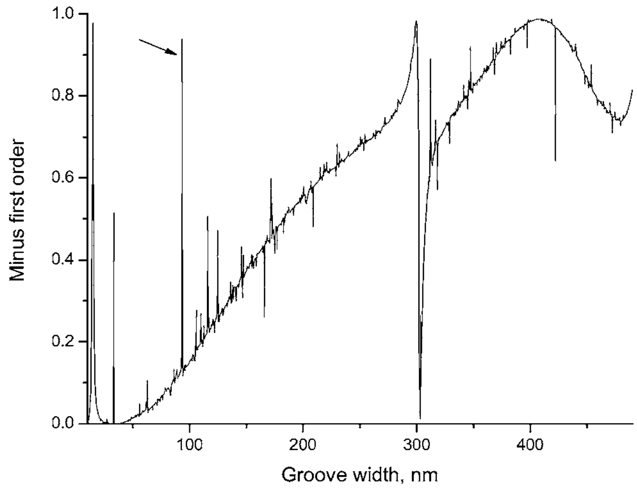

Fig. 1. Groove width dependence of the minus-first-order diffraction efficiency with $\lambda=632.8$ nm and $\Lambda=500$ nm.

Table 1. Complex Effective Index of a Few First- and Last-Order TMM and FMM Modes with Truncation Number $N=31$[a]

Mode order	True Modes		Fourier Modes	
	Real	Imag.	Real	Imag.
0	1.10459	0.0	1.10476	0.0
1	0.0	3.16773	0.0	3.23267
2	0.0	6.66824	0.0	6.99719
3	0.0	10.0311	0.0	10.0311
…	…	…	…	…
$N-6$	0.0	18.5053	0.0	20.5776
$N-5$	0.0	19.1612	0.0	23.9795
$N-4$	0.0	19.8468	0.0	26.1466
$N-3$	0.0	20.268	5.3312	0.0
$N-2$	0.0	20.5031	6.09379	0.0
$N-1$	0.0	21.1819	12.5095	0.0

[a] At the end of the FMM modal spectrum, there are three spurious modes having a character completely different from the corresponding true modes of the same order.

smooth baseline given by the TMM; a zoom on any low-noise section of the curve reveals that the noise is present everywhere.

The grating modes of the FMM are obtained as a solution of an eigenvalue problem by matrix diagonalization. The total number of considered modes is equal to the truncation number or to the matrix dimension. The grating modes of the TMM are the natural lamellar structure modes satisfying the actual boundary conditions, i.e., the dispersion equation of the true binary rectangular grating [10]. In what follows the effective index of a grating mode is defined as the ratio between the eigenvalue of an FMM or a TMM solution (i.e., the mode propagation constant normal to the structure plane) and the vacuum wavenumber $k_0=2\pi/\lambda$. In the present lossless structure the effective index of a propagating mode has a nonzero real part and a zero imaginary part, whereas the nonzero part of an evanescent mode is the imaginary part that is responsible for the mode field damping. The effective index of a propagating mode of plasmonic nature is real and larger than 1, whereas that of a propagating dielectric mode is real and smaller than the refractive index in the grooves (here less than 1).

Table 1 gives the list of the effective indices of the first and the last grating modes propagating up and down the grating grooves as given by the TMM and the FMM for a groove width of 93.518 nm and truncation number $N=31$. The chosen groove width corresponds to the strongest instability shown by the arrow in the graph of Fig. 1. The TMM modes are listed in decreasing order of the square of the real part of their effective index. The evanescent modes of midorder number are not relevant in the present analysis and are therefore left out. For a given groove width all TMM modes of the TM polarization are evanescent except the single plasmon mode of zeroth order. More complicated is the ordering of the list of the FMM modes. Table 1 reveals that all TMM modes up to order $N-3$ have an FMM mode counterpart, but at the end of the FMM modes spectrum there are a restricted number of modes of completely different character that do not have their TMM counterpart. This is undoubtedly the result of the truncation of the infinite matrices to be diagonalized. These modes will hereafter be called "spurious" modes, although they are needed to complete the set of eigenvectors for expressing a correct solution. It is remarkable that all these spurious modes have a plasmonic character since their effective index is real and larger than 1. This characteristic represents a first criterion for identifying them in the grating mode spectrum. Such modes propagate without attenuation in the case of a lossless metal.

Having identified the FMM modes without a TMM counterpart, we have analyzed how this group of modes evolves with increasing truncation number. The results are in Table 2, where the effective index of all plasmon-like modes found by the FMM is given with increasing truncation number. With the increase in truncation number it is found that TMM and FMM modes have their counterparts except for a few modes of order close to the truncation number. All common modes exhibit a regular convergence behavior as illustrated in Table 2 with the example of the plasmon mode of order zero. The FMM spurious modes behave very differently with increasing truncation number: there is no clear tendency in the evolution of their effective index. It is an interesting feature of the spurious modes that their unstable effective index is always notably larger than the true plasmon mode effective index. Once the fundamental plasmon mode effective index is known or even estimated, this feature can be used as a second criterion to identify them within the mode spectrum.

Figure 2 illustrates the transverse magnetic field distribution of a spurious plasmon mode and of the fundamental plasmon mode over one period across the grating grooves with a groove width of 93.518 nm. Unlike in the fundamental plasmon, the real and imaginary parts of the spurious modal field oscillate at the largest spatial frequency of the Fourier series, and their field has a larger amplitude in the metal ribbon. This again characterizes the spurious modes as modes of high order close to the truncation number, whereas their plasmon-like character would place them at the beginning of the modal

Table 2. Evolution of the Effective Index of the Spurious FMM Modes in a Lossless Metal Grating with the Truncation Number N[a]

Truncation Number	$N-1$	$N-2$	$N-3$	$N-4$	Mode 0
31	12.5095	6.09379	5.3312	—	1.10476
33	10.5525	7.30255	5.33273	6.347	1.10570
35	19.3175	18.8975	6.43998	6.00416	1.10520
37	11.8483	7.49204	5.98195	—	1.10423
39	36.0806	13.0032	7.77949	6.2364	1.10400
41	27.0125	16.1508	7.2718	6.89867	1.10455
43	12.2049	8.76289	6.73086	—	1.10506
45	16.4006	8.19296	7.2571	—	1.10496
47	15.017	8.60048	7.51235	—	1.10450
49	50.1534	13.6935	9.58697	7.57716	1.10428
51	20.7432	8.67485	8.37703	—	1.10449
53	72.2236	14.7316	9.98877	8.19877	1.10479
55	32.5439	16.1913	10.0785	8.52735	1.10483
57	26.8626	18.9459	9.70253	9.14669	1.10460
59	75.1167	15.2807	11.2021	8.97274	1.10443
61	26.7488	19.5400	10.5004	9.5878	1.10448
121	38.8897	32.1015	19.2355	18.3573	1.10459

[a]The last column gives the effective index of the regular plasmon mode as a reference.

spectrum and can be used as a third criterion for identifying them within the mode spectrum.

The appearance and behavior of spurious modes can be explained by the well-known Gibbs phenomenon [11,12]. The Fourier series at a jump discontinuity has large oscillations near the jump. The amplitude of oscillations is not reduced as the number of representing harmonics increases, but it approaches a finite limit. When the function changes sign at the jump (permittivity function in the case of a metal grating), such oscillations can increase the number of zero crossings of the truncated Fourier series. This corresponds physically to the inclusion of new metal-like layers in one grating period. Every additional metal layer supports at least one plasmon mode; thus the number of plasmon-like modes increases with the number of such artificial interfaces.

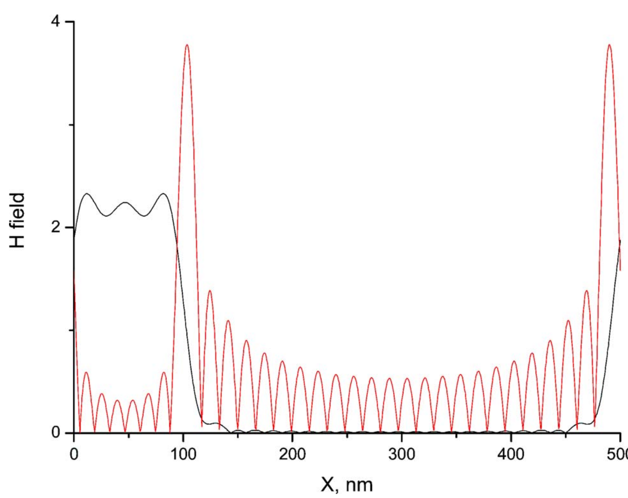

Fig. 2. (Color online) Example of FMM modal H field of mode $N-1$ (multi-peaked curve, red online) and regular plasmon mode 0 (lower curve, black) for the truncation number 31. The groove is located between $x=0$ and 93.518 nm.

Although such a consideration brings some light and helps explain the phenomenon, it does not deliver an explicit analysis of the problem. Together with the permittivity $\epsilon(x)$, the inverse pemittivity $1/\epsilon(x)$ as well as the field $H_y(x)$ are represented in the FMM by their Fourier series. The new technique of Maxwell's equation truncation of [1], which is a big step forward for the FMM, makes a physical interpretation even more involved. This all renders a fine modal analysis of the truncated Fourier transformed problem and of its spurious modes very complicated if not impossible.

Figure 3 illustrates the behavior of the spurious mode effective indices versus the groove width in the 210–290 nm interval (the largest range with the presence of four spurious modes). The truncation number is 31. It is clear that the mode effective index behavior is regular without any sign of instability unlike what one would expect from the noise on the minus-first-order diffraction ef-

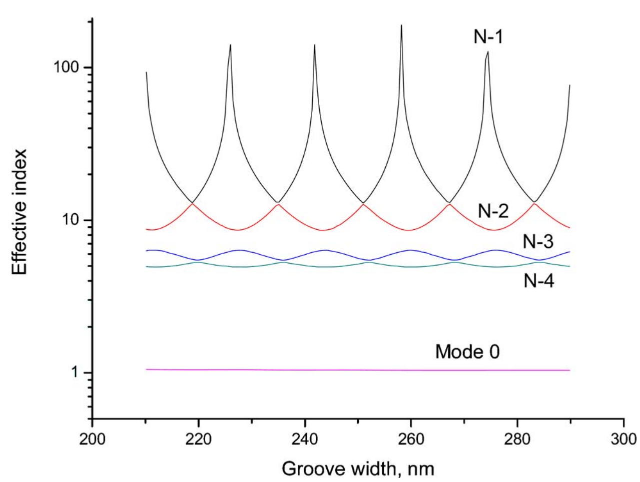

Fig. 3. (Color online) Effective index spurious modes dependence versus groove width.

ficiency in Fig. 1 in the same interval. This leads one to infer that the observed instabilities do not have a numerical origin but can be explained by an interference effect of the spurious modes in the grating layer.

This section can be concluded by the following statements:

- The "spurious" modes do not exist physically; they are a mathematical artifact due to the truncation of an infinite set of equations.
- The "spurious" modes appear only in structures where there is a transition from a dielectric to a metal character;
- The set of "spurious" modes is limited to a few members regardless of the truncation number; this property has been observed in structures having a wavelength scale period and should not be extrapolated without verification.

3. FOURIER MODE INTERFERENCE

From Tables 1 and 2 one sees that the spurious Fourier modes may have a very large effective index. These modes will consequently experience close to unity reflection at the grating layer interfaces because of the large impedance mismatch. For example, under the conditions of Table 1, mode $N-3$ experiences a power reflection coefficient into itself of 0.99 at the air interface and 0.997 at the bottom metal interface. This implies that there can be in the lossless metal case a very large energy accumulation for this mode between both grating layer interfaces if the Fabry–Perot resonance condition is fulfilled. Although the number of spurious modes is limited, the dependence of their effective index on the structure parameters and incident conditions is extremely sensitive and rather complicated; therefore one can expect a high density of sharp resonances. However, such resonances are not to be interpreted as noise; they do behave as resonances. Let us consider the example of an instability peak at the groove width of 93.518 nm and investigate its behavior in a short range of groove width from 93.4 nm to 93.6 nm. The diffraction efficiency represented in Fig. 4 reveals a typical true resonance curve without any sign of numerical instability. At any point of the graph in Fig. 1, a fine scan of the groove width reveals a high density set of resonances of different width and strength as shown in Fig. 5.

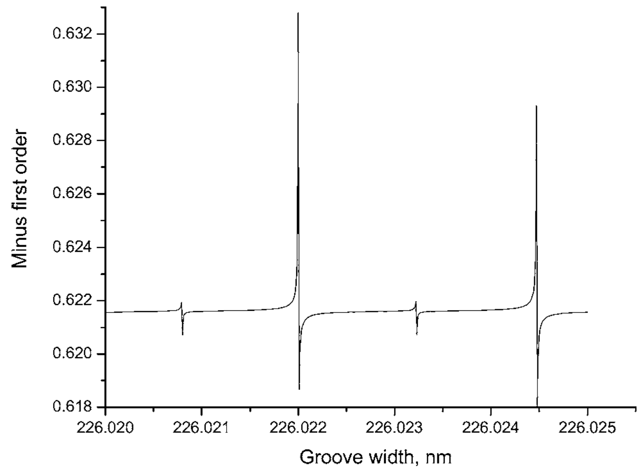

Fig. 5. Set of resonances under a fine scan of the groove width.

Figure 6 illustrates the resonant accumulation of energy resulting in a large H field amplitude inside the grating layer related with the spurious Fourier modes. The parameters correspond to the exact mode $N-3$ resonance position of Fig. 4. The H field distribution is typical for a standing wave inside a Fabry–Perot resonator. At the field peaks, the H field amplitude reaches as much as 67 times the incident field amplitude. This anomalously strong field enhancement is dramatically illustrated by the scale of the 3D graph, where the incident field pattern for $z<0$ appears to be flat and close to zero and where all other modal fields are by far dominated by the mode $N-3$ resonance. The fact that there is a large field amplitude in the ideal metal region highlights the nonphysical character of such artificial solution.

At this stage it can be concluded that the instabilities exhibited in Fig. 1 have nothing to do with numerical artifacts. They are simply and meaningfully the consequence of the Fourier mode interference in the grating layer. The effective index of such modes is so large and their Fabry–Perot resonance in the grating depth is so strong with so high a quality factor that the least change

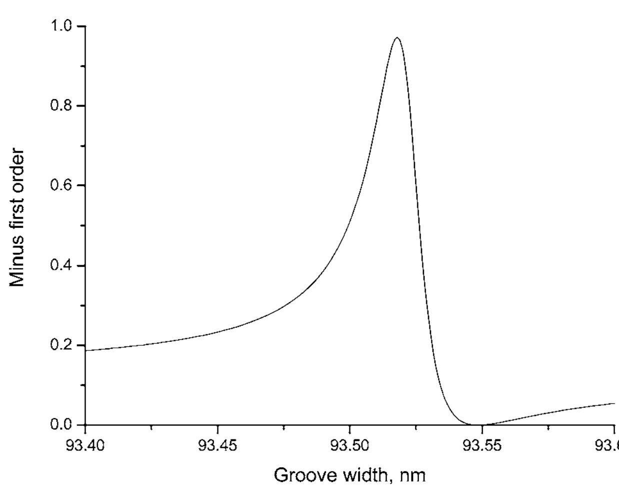

Fig. 4. Resonance effect of spurious Fourier mode $N-3$ self-interference in the grating layer.

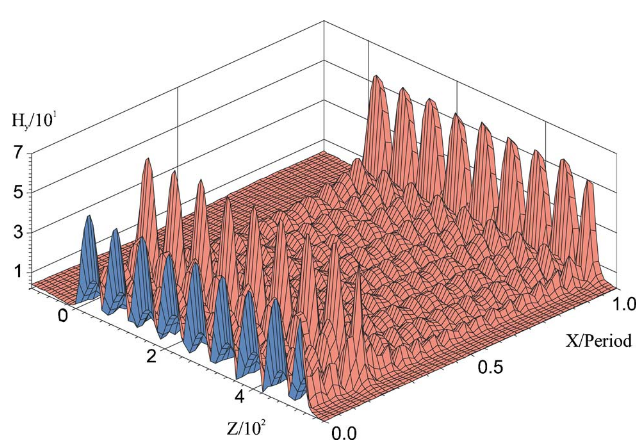

Fig. 6. (Color online) Field enhancement in the grating region under spurious mode resonance. The air groove is located between 0 and 0.187 of the X/period axis.

of depth or of line/space ratio or in wavelength leads to the suppression of the observed resonance, or possibly to the resonance of another spurious mode or to the coupling between two such modes. The noisy curve of Fig. 1 thus represents the exact solution of the considered mathematical problem with a given size of truncated matrix containing the coefficients of the differential system.

4. CURING THE FOURIER MODAL METHOD FOR METAL–DIELECTRIC STEP PERMITTIVITY PROFILES

The modal phenomenology of the previous section sheds light on what the FMM actually does when it fails to deliver the exact solution of the step permittivity profile of a metal–dielectric structure. This does not yet provide the path from the noisy pattern of Fig. 1 to the smooth curve provided by the referenced TMM.

Popov *et al.* [6] have suggested artificially adding some absorption in the grating structure to damp the instabilities. From the above consideration it is clear why such intuition does lead to an improvement: with large enough absorption the propagation length of the spurious modes will decrease, as for instance that of a real short-range plasmon, with a resulting decrease of the corresponding Fabry–Perot quality factor and of the contrast of the noisy interference pattern. With the modal understanding gained in the previous section it is now possible to address the problem anew and find out a finer, and at the same time more general, solution. Since the spurious modes are the effect of the truncation of the infinite matrix containing the coefficients of the differential system in combination with the permittivity step transition from dielectric to metal character, the problem can be expressed as "What should be kept of these modes to ensure continuity toward the true solution?" Leaving aside a single one of these spurious modes in the field-matching equations leads to a wrong solution because the eigenmode set becomes incomplete. As Table 2 suggests, and as Fig. 2 confirms, these spurious TM modes exhibit an oscillatory character with a spatial frequency that is related to the spatial frequency of the highest-order harmonics considered in the truncated system. Thus, these modes are located at the end of the modal spectrum, and for this reason one can reasonably expect that with the increase in the truncation number these modes should play a decreasing role in the convergence process. This intuitive reasoning leads us to keep the spurious plasmon modes for the sole purpose of the field matching and to forbid them to propagate through the grating layer in order to exclude their unpredictable high-contrast interference effect. This implies that the spurious plasmon mode amplitudes are set to zero once they have been used in the interface field-matching equations. In other words, the loss factor of these modes is set to infinity. Applying this spurious mode management to the structure of Fig. 1 with the FMM gives the diffraction efficiency curve of Fig. 7, where there is no longer a trace of any instability and the results are very close to those given by the reference TMM.

Figure 8 presents the difference of minus-first-order order diffraction efficiency calculated by the TMM and the FMM considering 31 and 61 modes and shows that the suggested mode management enables the FMM to converge toward the exact reference result.

Figures 9 and 10 illustrate the H field distribution inside the grating region under the conditions of Fig. 6 with mode filtering in the FMM (Fig. 9) and calculated by the

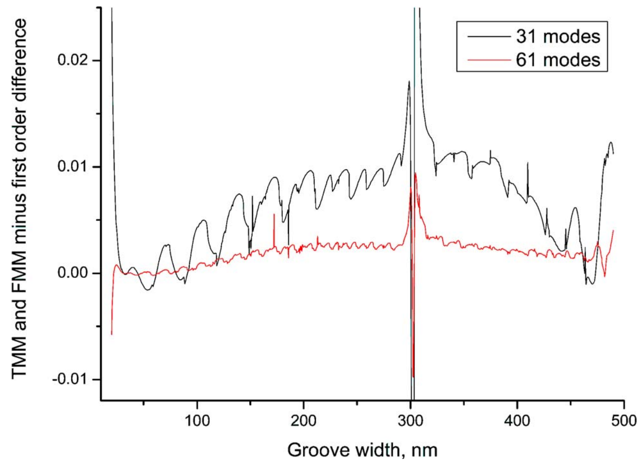

Fig. 8. (Color online) Difference of diffraction efficiencies calculated by TMM and FMM for 31 (upper curve, black) and 61 modes (lower curve, red online).

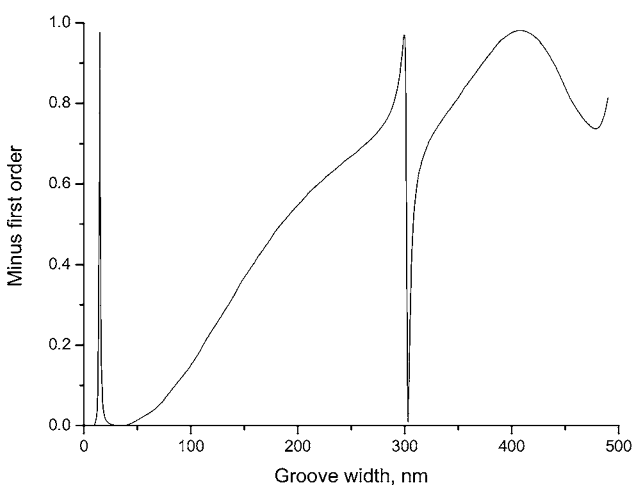

Fig. 7. Diffraction efficiency of the minus first order calculated by the FMM with the described spurious modes filtering.

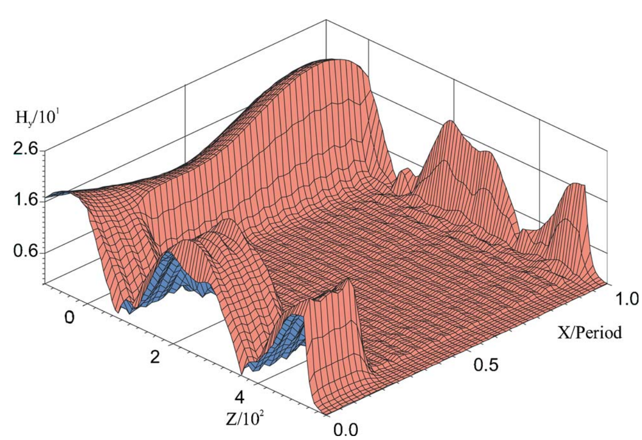

Fig. 9. (Color online) H field distribution in the grating region calculated by the FMM with mode filtering.

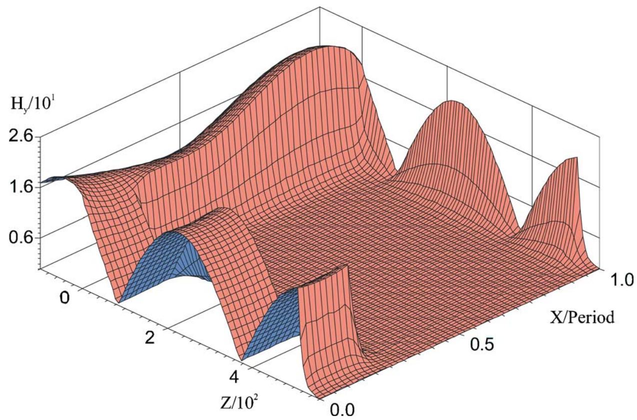

Fig. 10. (Color online) H field distribution in the grating region calculated by the reference TMM.

reference TMM (Fig. 10). These figures show that the two methods give a close to identical field distribution, but that the field calculated by the FMM still exhibits a bumpy character, while the field calculated by the TMM has a smooth and physically correct shape. The suppression of the spurious mode resonances thus leads to the actual physical field distribution inside the grating region. In contrast to Fig. 6, the field inside the ideal metal region in Figs. 9 and 10 is now close to zero, and it is clear that the remaining standing-wave field character in the grating region is due to the Fabry–Perot resonance of the fundamental plasmon mode.

We have so far identified and characterized the Fourier modes responsible for the observed instabilities of the FMM, we have explained the high-contrast interference and resonance mechanisms involved, and we have suggested a mode-filtering principle permitting the suppression of the instabilities while still satisfying the boundary conditions of the electromagnetic problem. Unlike in [6,7] where the structure as a whole is made more lossy, which affects all modes, the present approach is highly selective and treats the actual electromagnetic problem. The development of a safe filtering algorithm can now be undertaken on the basis of the following mode selection criteria: (1) The spurious modes are always very slow waves; therefore the only modes with which there may be confusion are the true plasmon modes. (2) Their effective index is much larger than that of a true slow wave plasmon. (3) Their propagation constant is always extremely sensitive to any change of parameter unlike that of the true plasmon modes. (4) Their field always has the largest spatial frequency corresponding to the truncation number. (5) Their field has high amplitude and high spatial frequency in the metal parts.

5. SUPPRESSING THE FOURIER MODAL METHOD INSTABILITIES FOR ARBITRARY METAL–DIELECTRIC PROFILES

The unpredictable high-contrast interferences of spurious modes as well as between them is dangerous in the case of nonlamellar metal or metal–dielectric gratings of an arbitrary groove profile where the slicing technique is used, as is most often the case. In such a general case the grating layers are rather thin, but high-quality Fabry–Perot effects persist even in the case of lossy metals for two reasons: First, the effective index of the spurious modes can be so large that the Fabry–Perot modes might not all be cut off. Second, the slices are usually so thin that the spurious modes' damping coefficient may be small enough to permit resonances within the slice. The persistence of spurious mode resonances in thin lossy metal grating slices is clearly evidenced in Fig. 11, showing the diffraction efficiency of the minus first order in a binary grating layer of 20 nm thickness only under the excitation conditions and same period as in Fig. 1. The metal refractive index is $0.5+i10$. This case is ten times more lossy than that considered in [7]; nevertheless, the diffraction efficiency still reveals strong interference instability. Figure 11 shows that the suggested spurious mode filtering completely removes the instabilities. This thin-grating result implies that the approach suggested in [6], consisting of introducing higher artificial losses in the structure, would lead here, as well as in the case of the sliced arbitrary profile hereunder, to a persistence of the instabilities.

Having evidenced the role of spurious modes in a thin lossy slice, we now consider a complete nonlamellar grating groove. The chosen example is that of a sinusoidal metal grating profile because there is for this profile an exact reference solution by application of the C method [13,14]. The smooth sinusoidal profile will be cut up into a number of horizontal slices. A complex refractive index of $n_s=0.5+i10$ is considered, which is very close to the gold refractive index at the incident wavelength of 1550 nm. The grating period is 1500 nm, and the peak-to-trough grating depth is 500 nm. The incident angle is 30 deg under TM polarization. The chosen number of slices of 10 nm thickness is 50. The diffraction efficiency of the minus first order versus the number of modes (truncation number) is presented in Fig. 12 for the FMM method without (middle curve, red online) and with (lower curve, blue online) the suggested mode filtering and for the TMM method (upper curve, green online). The horizontal line corresponds to the reference value of the diffraction efficiency of a sinusoidal grating calculated by the C

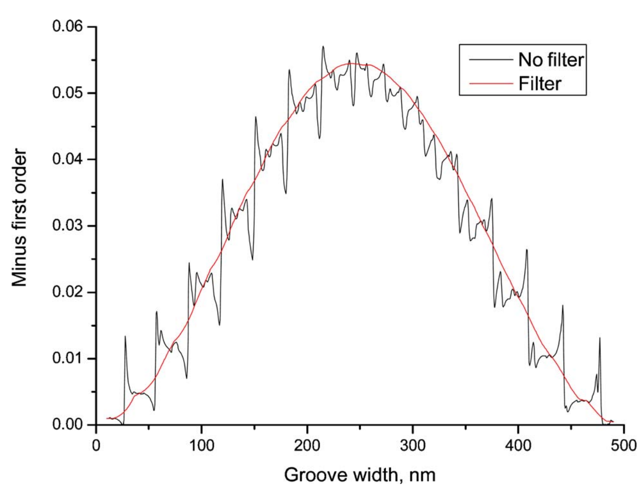

Fig. 11. (Color online) Diffraction efficiency of the minus first order of a 20 nm thin lossy metal grating without (noisy curve, black) and with (smooth curve, red online) spurious modes filtering.

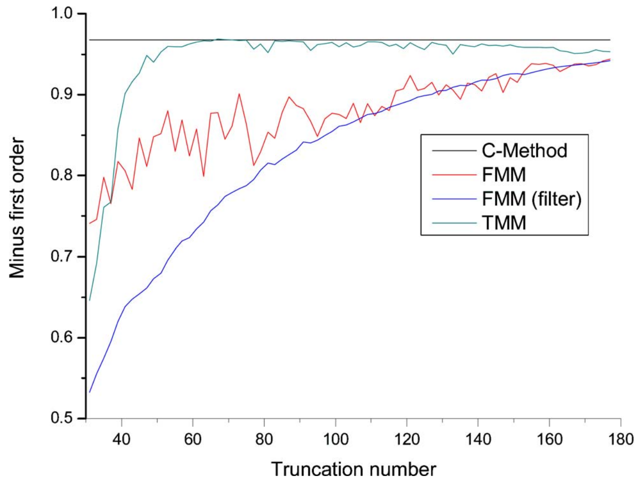

Fig. 12. (Color online) Diffraction efficiency of the minus first order of a sinusoidal grating calculated by the C method (horizontal line) and for a sliced grating calculated by the FMM without (middle curve, red online) and with (lower curve, blue online) spurious modes filtering and calculated by the TMM (upper curve, green online).

method. It is worth noting that the C method requires only ±7 orders (15 Fourier modes) to provide 10^{-8} accuracy.

This last figure, representing the convergence rate of the different methods, teaches us the following:

- The interference of spurious modes in sliced metal gratings provokes instabilities in the convergence curve even in the case of lossy metals in the near-infrared spectrum.
- The suggested spurious mode filtering ensures a smooth convergence curve and offers the possibility of using asymptotic methods to improve accuracy of the result.
- The initial convergence rate of the TMM in a sliced grating is much faster than that of the FMM.

It should be pointed out that the example of a sinusoidal grating as a nonlamellar profile was chosen here only because it permits a comparison with a reference method. A sinusoidal profile is actually not the type of profile for which a slicing modal method is best adapted because of the presence of corners resulting from the staircase approximation and especially of the nonrealistic duty cycle of the first and last slices. The question of the convergence rate among the three considered modal approaches should consequently not be considered as settled by this numerical experiment, the main teaching in Fig. 12 being that of the persistence of the instabilities in nonlamellar profiles even in the presence of lossy metals and their removal by means of the proposed filtering principle. The convergence behavior of the TMM versus the number of slices and the number of modes in a sinusoidal metal grating has been exhaustively investigated [15] and will be reported elsewhere.

6. CONCLUSION

The above modal analysis of the Fourier modes shows that the failure of the Fourier modal method (FMM) to provide reliable results in the case of metal–dielectric gratings under TM incidence cannot be accounted for by numerical instabilities. These instabilities are actually the deterministic result of the interference, coupling, and resonance effects of plasmon-like Fourier modes generated by the truncation of the infinite matrix containing the coefficients of the differential system. The solution of this system is highly sensitive to the optogeometrical grating parameters because the involved spurious modes are very slow waves of very high spatial frequency experiencing high reflection at the border of the grating region and grating slices.

The present modal analysis of the problems faced by the rigorous coupled-wave analysis (RCWA) or the FMM also gives a hint as to how to process these spurious modes in the objective of getting close to the exact solution while removing the instabilities. It was found on the basis of a sole physical rationale, but without mathematical demonstration, that keeping the spurious modes for satisfying the boundary conditions and forbidding their propagation suppresses the instabilities completely and permits a smooth, although slow, convergence toward the exact solution.

It was also shown that the instabilities persist in shallow gratings and, most important, in arbitrary profile metal–dielectric gratings in the presence of lossy metals, and that the proposed filtering principle suppresses the instabilities.

It can be considered that the field of usability of the FMM or the RCWA has now been opened to arbitrary 1D gratings under arbitrary incidence conditions. The true-mode method remains the reference method for metal–dielectric structures under TM incidence. It also provides very quickly and with a restricted number of modes a result that is close to the exact solution.

The comparison between methods that has been achieved in the present paper has the character of an objective and up-to-date comparison in that the different methods have been implemented with their last known improvements and that they have been homogeneously implemented at an identical level of highly professional coding methodology and skills. The reader may check the results of this paper by using the free codes available at www.mcgrating.com.

ACKNOWLEDGMENT

The authors are grateful to Maud Sarrant-Foresti, of Saint-Gobain Recherche, Paris, for her contribution to the finalization of the 1D true-mode method, which has served in the present comparison. This paper is a contribution of O. Parriaux and A. V. Tishchenko to a modeling benchmarking action in the Network of Excellence of the European Commission on Microoptics (NEMO).

REFERENCES

1. P. Lalanne and G. M. Morris, “Highly improved convergence of the coupled-wave method for TM polarization,” J. Opt. Soc. Am. A **13**, 779–784 (1996).
2. L. Li, “Use of Fourier series in the analysis of discontinuous periodic structures,” J. Opt. Soc. Am. A **13**, 1870–1876 (1996).
3. G. Granet, and B. Guizal, “Efficient implementation of the

coupled-wave method for metallic lamellar gratings in TM polarization," J. Opt. Soc. Am. A **13**, 1019–1023 (1996).
4. M. Nevière and E. Popov, *Light Propagation in Periodic Media: Differential Theory and Design* (Marcel Dekker, 2003).
5. E. Popov and M. Nevière, "Grating theory: new equations in Fourier space leading to fast converging results for TM polarization," J. Opt. Soc. Am. A **17**, 1773–1784 (2000).
6. E. Popov, B. Chernov, M. Nevière, and N. Bonod, "Differential theory: application to highly conducting gratings," J. Opt. Soc. Am. A **21**, 199–206 (2004).
7. K. Watanabe, "Study of the differential theory of lamellar gratings made of highly conducting materials," J. Opt. Soc. Am. A **23**, 69–72 (2006).
8. L. C. Botten, M. S. Craig, R. C. McPhedran, J. L. Adams, and J. R. Andrewartha, "The dielectric lamellar diffraction grating," Opt. Acta **28**, 413–428 (1981).
9. L. C. Botten, M. S. Craig, R. C. McPhedran, J. L. Adams, and J. R. Andrewartha, "The finitely conducting lamellar diffraction grating," Opt. Acta **28**, 1087–1102 (1981).
10. M. Foresti, L. Menez, and A. Tishchenko, "Modal method in deep metal–dielectric gratings: the decisive role of hidden modes," J. Opt. Soc. Am. A **23**, 2501–2509 (2006).
11. J. W. Gibbs, "Fourier series," Nature **59**, 200 (1898).
12. J. W. Gibbs, "Fourier series," Nature **59**, 606 (1899).
13. J. Chandezon, M. T. Dupuis, and G. Cornet, "Multicoated gratings: a differential formalism applicable in the entire optical region," J. Opt. Soc. Am. **72**, 839–846 (1982).
14. T. Vallius, "Comparing the Fourier modal method with the C method: analysis of conducting multilevel gratings in TM polarization," J. Opt. Soc. Am. A **19**, 1555–1561 (2002).
15. M. Foresti, "Etude et développement de systèmes nanostructurés pour verres optiquement fonctionnels," Ph.D. thesis (Université Jean Monnet, Saint-Etienne, 2007).